Title
Particle-in-cell simulations of intense laser pulses coupling into plasma channels

Authors
Dimitrov, D.A.
Bruhwiler, D.L.
Cary, J.R.
et al.

Publication Date
2004

Particle-in-cell simulations of intense laser pulses coupling into plasma channels

D. A. Dimitrov[*], D. L. Bruhwiler[*], J. R. Cary[*†], P. Messmer[*], C. Geddes[**], W. Leemans[**] and E. Esarey[**]

[*]*Tech-X Corporation, 5621 Arapahoe Avenue, Suite A, Boulder, Colorado 80303*
[†]*Physics Department, University of Colorado, Boulder, Colorado 80309-0390*
[**]*Lawrence Berkeley National Laboratory, University of California, Berkeley, California 94720*

Abstract. The guiding of intense laser pulses in plasma channels is necessary to maximize the energy of electrons accelerated in a laser wakefield accelerator. A significant fraction of the energy in the laser pulse may be lost during and after coupling from vacuum into a channel. For example, imperfect coupling can lead to enhanced leakage of laser energy transversely through the channel walls. We present 2D particle-in-cell (PIC) simulations, using the VORPAL code [1], of an example problem. We present a numerical diagnostic, based on simultaneous FFT's in space and time, which enables quantitative measurements of forward and backward propagating pulse energy and its spectra. Future work will be directed toward VORPAL parameter studies designed to optimize the amount of laser energy that couples into a channel.

INTRODUCTION

Laser wakefield accelerators (LWFA) can sustain electron plasma waves with longitudinal electric fields on the order of 100 GV/m [2]. However, the distance over which electron beams can be effectively accelerated in an LWFA is limited by the length over which a focused laser beam can be propagated, unless an efficient laser pulse guiding is implemented. A preformed plasma density channel with a parabolic transverse profile can be used as one approach for optical guiding of short intense laser pulses [3, 4].

In the best case, most of the energy in the laser pulse driving an LWFA is gradually lost to the plasma wake. This energy loss is called pump depletion. Other sources of energy loss – including laser instabilities, leakage through the walls of the channel, and backward Raman scattering–reduce the efficiency of the LWFA and the maximum energy of the accelerated electrons.

Correct numerical diagnosis of these diverse processes in a PIC code requires a technique that can unambiguously determine how much electric and magnetic field energy is propagating forward or backward on the grid, within a range of frequencies and wavenumbers near the central values for the laser pulse.

We demonstrate here, using VORPAL [1] simulations of a laser pulse entering a preionized channel, that simultaneous FFT's in space and time can provide this diagnostic. In particular, we are able to identify the leakage of pulse energy transversely through the channel walls and obtain an approximate upper limit on pump depletion over the course of a density ramp one Rayleigh length long, and also during subsequent propagation of

the pulse down the channel for another Rayleigh length.

DIAGNOSTICS FOR SIGNAL WAVEVECTOR AND FREQUENCY DETERMINATION

We apply Fast Fourier Transforms (FFTs) in both space and time on components of the total electric field in the simulation box and then calculate the power spectral density (PSD) to determine existing wave signatures in the electric field. The power spectral density is defined as the modulus squared of the Fourier transform of a signal. We consider here Fourier transforms of electric field components $E_\alpha(\mathbf{r},\, t)$, where α is equal to x, y, or z. The PSD in this case is $|E_\alpha(\mathbf{k},\, \omega)|^2$, where $E_\alpha(\mathbf{k},\, \omega) = \int E_\alpha(\mathbf{r},\, t)\exp(-i(\mathbf{k}\cdot\mathbf{r}-\omega t))\,d\mathbf{r}dt$. The position of observed PSD peaks in $(\mathbf{k},\ \omega)$ space indicate the wavevector and frequency of excited waves. We calculate the integral (sum) of the power spectral density, the total power in the signal, to estimate pump depletion and leakage. Moreover, the location of the power spectrum peaks in the $(\mathbf{k},\ \omega)$ space allows to distinguish the direction of propagating wave signals in real space.

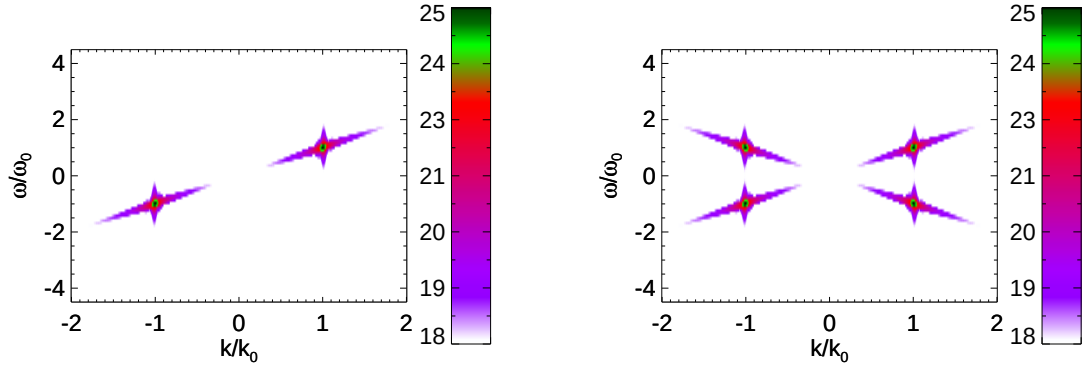

FIGURE 1. Images of the logarithm of the PSD for two simulation cases in vacuum. The left plot is for a laser pulse propagating along the $(1,\ 0)$ direction and the peak in the first quadrant is at the pulse wavevector k_0 and frequency ω_0. The peak in the third quadrant is from an FFT that is a *c.c.* image of the PSD from the first quadrant. The right plot shows two counter-propagating pulses. This diagnostic provides a direct capability to detect and distinguish forward and backward moving signals.

We demonstrate this capability for a simulation in which we launch laser pulses in vacuum in different directions. The VORPAL code allows launching pulses from any boundary of the simulation box in any direction. The pulse could have different envelope funcions, focus location, and width at focus. These are parameters controled from a simulation's input file. We consider two-dimensional (2D) simulations here. Linearly polarized pulse, along the ignorable direction, is loaded in the simulations using the functional form [5, 6]

$$E(x,\, y) = E_0\sqrt{\frac{W_0}{W(x)}}\exp\left(-\frac{y^2}{W^2(x)}\right)\cos\left(k_0 x-\omega_0 t+\frac{k_0 y^2}{2R(x)}-\phi(x)/2\right)env(x)\,, \tag{1}$$

where the width of the pulse is $W(x) = W_0\sqrt{1+\left(x-x_f\right)^2/Z_R^2}$, x is the direction of the pulse propagation, W_0 is the width at the location of focus x_f, $Z_R = k_0 W_0^2/2$ is the Rayleigh length, k_0 and ω_0 are the wavevector and (angular) frequency of the pulse, E_0 is the field amplitude, $env(x)$ is the pulse longitudinal envelope function which for the simulations here is a half sine function, $R(x) = x - x_f + Z_R^2/(x-x_f)$, and $\phi(x) = \tan^{-1}\left(\left(x-x_f\right)/Z_R\right)$.

If we do an FFT in space along the longitudinal axis x, for a line though the middle of the pulse (the line $y = 0$ in the simulations) and an FFT in time, then a pulse moving forward will show peaks in the PSD plot at $(k_0,\ \omega_0)$ and at $(-k_0,\ -\omega_0)$ since the PSD of a real function is even. The appearance of these peaks in the calculated logarithm of the PSD (only the top seven orders of magnitude are shown) for a pulse moving along the $(1,\ 0)$ direction is shown on the left plot in Fig. 1. The simulation box had $N_x = 2400$ cells along x. The values of the E_z component of the field, the polarization direction, were FFTd in space using all 2400 points along the line $y = 0$ although the pulse occupies approximately 600 cells at any instance of time. In contrast, the number of time data points used for the FFT along the time axis was 200. For all other results presented here, except the ones in Fig. 1, the number of time samples was 128. The time data were collected dumping the electric field every N_t number of time steps, starting at specific time in the simulation. Both, the time samples and the cell spacing of the simulation grid were chosen to resolve the pulse wavevector and frequency. The cell size was chosen such that a pulse wavelength is sampled at least 16 times if sampled at consecutive cell points. The resolution along the time axis was chosen in the same way. However, since we FFTd only over 128 or 200 sample points in time, the resolution in frequency space is smaller than in wavevector space. We used a Hanning window in all FFTs along the time axes to suppress the Gibbs phenomenon since at the end points of the time sampled data, the signal in the transformed data usually starts from a non zero value.

The plot on the right in Fig. 1 shows two counter propagating laser pulses. One was launched from the left boundary of the simulation box, $x = 0$, and the other from the right one, $x = N_x\Delta x$. Now, in addition to the peak from the forward propagating pulse, there are the peaks of the backward propagating pulse in the second quadrant at $(-k_0,\ \omega_0)$ and its symmetric image at $(k_0,\ -\omega_0)$.

Note that if we had a pulse propagating backwards in time and forward in space, it will show the same peak locations. Moreover, if we calculate analytically the Fourier transform of Eq. (1), assuming that $W(x)$, $R(x)$, and $\phi(x)$ vary slowly over a pulse period and are taken as constants, then the peaks in Fig. (1) show fine structure. The resolution along the wavevector direction will show this structure if we zoom at the location of one the peaks. The resolution along the frequency axis should be increased to resolve the fine structure along it.

The extension of this diagnostic to estimate leakage from the channel and pump depletion is discussed in the next section together with the main simulation results.

EFFICIENT COUPLING IN PREIONIZED PLASMA CHANNELS

We selected representative parameters, similar to experimental ones for a LWFA, to study pump depletion and leakage when coupling and propagating laser pulses in preionized plasma channels. The pulse is launched in a vacuum region with length equal to the length L of the pulse. Then, the pulse enters a plasma cosine channel ramp with the profile (on average, the loader uses a bit-reversed algorithm)

$$n(x,\, y) = \frac{1}{2}\left(1 - \cos\left(\pi\left(x - x_0\right)/L_{ramp}\right)\right)\left(n_0 + \frac{\Delta n}{2}\cos\left(\pi\left(|y| - y_0\right)/y_0\right)\right) \qquad (2)$$

for $x_0 \leq x \leq L_{ramp}$ with L_{ramp} the length of the ramp. The term, $\cos\left(\pi\left(|y| - y_0\right)/y_0\right)/2$ is replaced with unity which is its value at $y = y_0$, for $y_0 \leq y \leq y_{max}$, where $y_{max} \geq y_0$ extends either to the transverse boundaries of the simulation box (wide walls), or is set to a smaller value to study guiding in channels with narrow walls. The plasma density in the channel, for $x \geq L_{ramp}$, is $n_0 + (\Delta n/2)\cos\left(\pi\left(|y| - y_0\right)/y_0\right)$ and $n_0 + \Delta n$ for $y_0 \leq y \leq y_{max}$. The axis of the channel is along the line $y = 0$. There are known matching conditions for Gaussian envelope pulses guiding in parabolic channels that specify values for the n_0 and Δn plasma density coefficients [2]. We have used here these conditions for n_0 and selected a larger value for Δn. Our channel is parabolic only for $y/y_0 \ll 1$. Results from simulations with a parabolic channel and a Gaussian pulse envelope longitudinally will be presented elsewhere.

The length of the ramp is a quantity that we varied in the simulations to understand its effect on coupling a pulse into channels with different ramp lengths. We considered simulations with ramp lengths of Z_R and $3Z_R$. The width of the channel transversely reaches its maximum value at a distance of $y_0 = 6\ \mu m$ from the axis of the channel. This is set equal to the width of the pulse at focus W_0 to achieve optimal guiding [2]. We also varied the transverse shape of the channel. We considered a channel with wide walls that extend to the boundaries of the simulation box, shown in the top row of plots in Fig. (2), and with narrow walls that extend for $1.5\mu m$ when the maximum value of the plasma density is reached in the transverse direction, the bottom row of plots in Fig. (2). These plots also show the excited plasma density wave due to the ponderomotive force which drives the wakefield.

The behavior of the wakefield for a pulse guided in a plasma channel from a representative run is shown in Fig. 3. The laser pulse had a length of 50 fs full width at half maximum (FWHM) which for a half sine pulse leads to a total length of 30 μm. The wavelength was set to $0.8\ \mu m$ and the width at focus to $6\ \mu m$ leading to a Rayleigh length of approximately 141 μm. We used $n_0 = 1.24 \times 10^{18} cm^{-3}$ and $\Delta n = 4.00 \times 10^{18} cm^{-3}$. In all simulations, the pulse is loaded from the left boundary with its focus set at the location of the fully formed channel, i.e. on top of the ramp. Note, however, that the location of the focus was calculated assuming the pulse propagates in vacuum. Due to the interaction with the plasma in the channel ramp, the focus will not be positioned exactly as in the vacuum case. This location mismatch will decrease the pulse power that couples in the channel and is part of the reason for the diagnostic we developed. The simulations with a Z_R ramp were done with a 6560×380 grid. The transverse length of the grid was chosen such that its half width is greater than or equal to $3W(0)$ to sufficiently

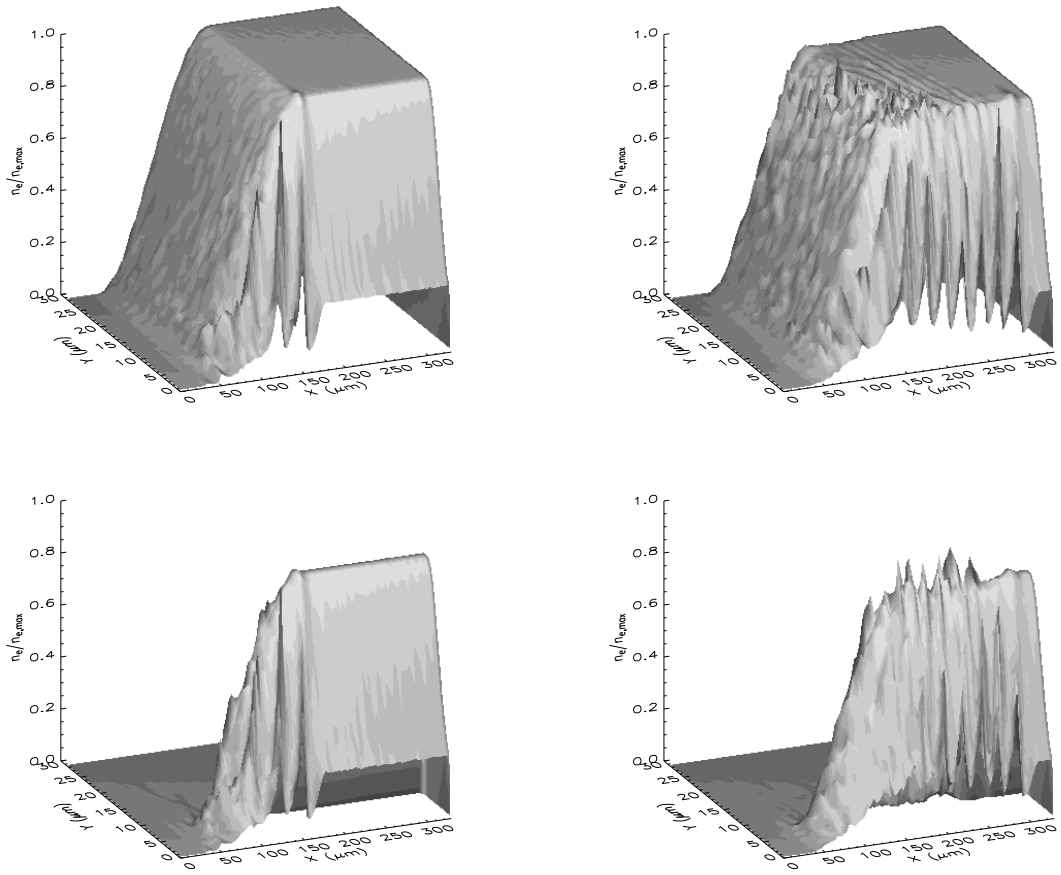

FIGURE 2. Normalized electron density in pre-ionized plasma channels with one Z_R cosine ramp. The plots show only half of the channels for $y > 0$ since the initial density is symmetric under the transform $y \rightarrow -y$. The top row of plots shows a channel with "wide" walls that extend to the transverse boundaries of the simulation box. The left plot is at the time the laser pulse has traveled through the ramp. The right plot is after the pulse has traveled a distance of Z_R in the channel. The bottom row of plots correspond to the same cases as the top row except that the channel has "narrow" walls. The pulse has traveled through the ramp, one Z_R, in the left column of plots and one more Rayleigh length in the completely formed channel in the right column of plots. In both cases, the excited plasma density wave is observed as expected.

cover the transverse width of the pulse at its maximum value at the loading boundary. Choosing similarly, the simulations for the channel with a $3Z_R$ ramp were done on a 9091×808 grid. In both cases the cell sizes were $\Delta x = 0.05\ \mu m$ and $\Delta y = 0.15\ \mu m$. The time step was chosen to satisfy the Courant condition. The smallest time step we used was $\Delta t = 0.118\ fs$.

All the simulations were run in parallel. In all simulations, a moving window algorithm was used to move the simulation box at the speed of light following the propagation of the laser pulse. All the large runs (with a $3Z_R$ ramp) were done on the IBM SP supercomputer at NERSC while most of the smaller runs (with a Z_R ramp) were done on the Tech-X linux cluster. These runs generate gigabytes (GB) of data files for each

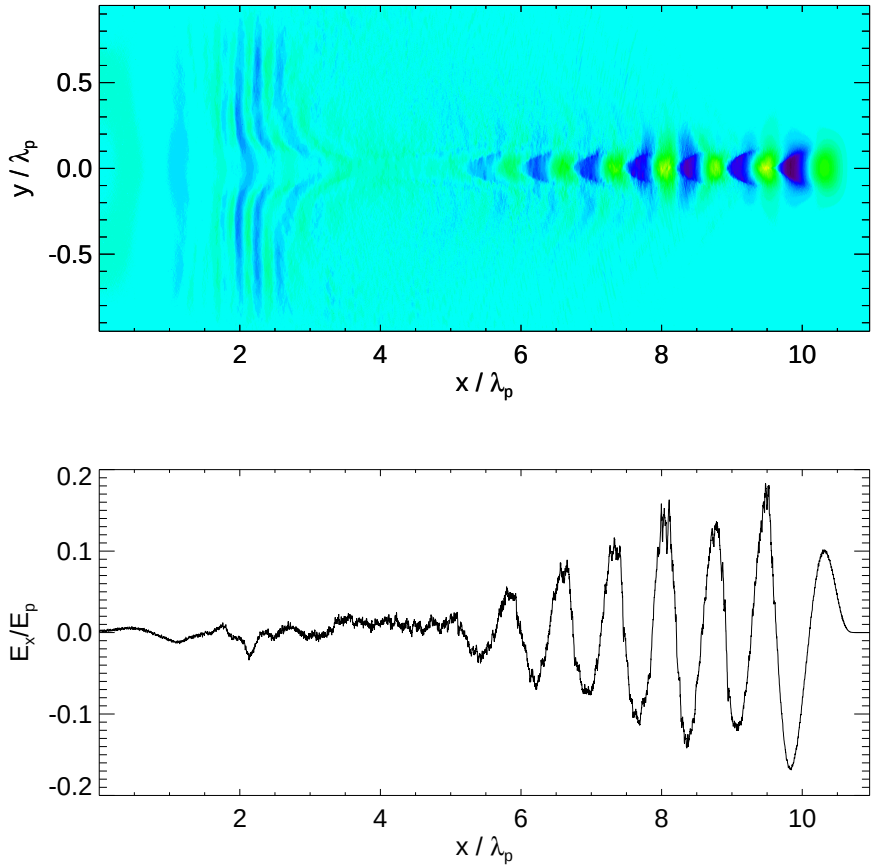

FIGURE 3. Wakefield, E_x, evolution in a channel with one Z_R ramp. The pulse has propagated through the ramp and a Z_R in the channel. The contour plot (top) of the wakefield clearly displays the passage of the pulse through the ramp on the left and then in guiding in the channel. The bottom plot shows a lineout of E_x through the axis of the channel.

scheduled dump in the simulations. The larger runs generate single-file particle dumps as large as (or somewhat larger than) 6 GBs which cannot be handled on 32 bit architectures and operating systems. The IBM SP machine at NERSC is a 64 bit architecture which is supported by the operating system. This allowed us to perform the large runs there.

The algorithm we implemented to estimate pump depletion and leakage from the channel with the PSD diagnostic consists in the following. For a specified rectangular region on the simulation grid, chosen such that the pulse is fully contained in it, the field data is dumped every N_t time steps for a total of 128 dumps. The spatial region of each data dump is used for the spatial FFT and the data in time from the 128 dumps is used for the FFT in time. The diagnostic is calculated in a post-processing mode after the field data dumps are generated. The freedom to select a spatial region for FFT allows us to concentrate only on the power spectrum from a sub region of the simulation box such as the domain of the channel where the pulse is or in the domain of the excited plasma

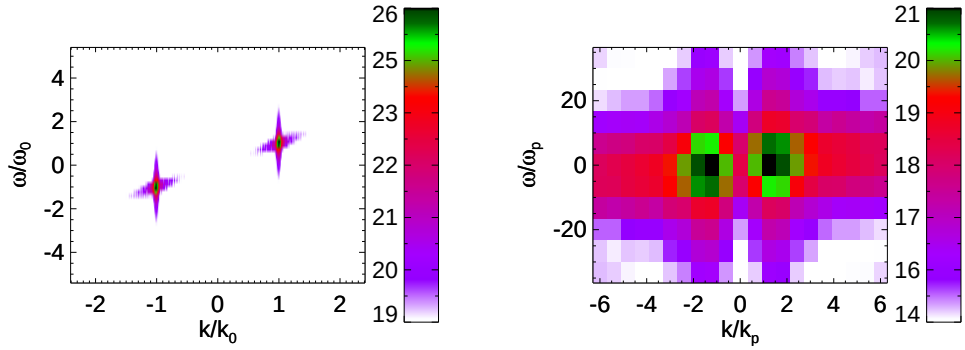

FIGURE 4. The left plot shows the logarithm of the integrated PSD of E_z, truncated at seven orders of magnitude from its maximum value. At this level of precision, only the forward moving signal is detected. The other plot represents the same quantity calculated for E_x and zoomed at the origin to detect the excited plasma wave. The chosen sampling rate in time, which is appropriate for the pulse signal, does not provide sufficient resolution for the plasma wave.

wave, in the wake.

The FFT in space is done on data along lines with $y = Const$ to detect longitudinally propagating waves or along lines with $x = Const$ to consider transversely excited signals. In both cases, these lines are in the selected spatial region for the PSD analysis. After the PSDs are calculated, they are summed first over all spatial lines used and then over a specified region of the calculated data points $(k_i,\ \omega_j)$ in wavevector-frequency space to obtain the total spectral power in a field component. The choice of a region in the $(k,\ \omega)$ space gives the freedom to study only forward propagating waves (if we sum only over $(k_i,\ \omega_j)$ points in the first quadrant of the $(k,\ \omega)$ plane) or only backward propagating signals (for a sum of wavevector-frequency values in the second quadrant).

We estimated the pump depletion in the channel by comparing the total power spectrum calculated over a region with $-y_{max} \leq y \leq y_{max}$ to the total power spectrum of a pulse in vacuum at focus calculated over the a spatial region with the same size and number of time samples. The value of y_{max} was chosen to cover the full transverse width of the simulation region when calculating the total spectral power from E_z. We sampled in time every simulation time step to obtain approximately the same number of data points in a pulse period as the number of spatial points over a pulse wavelength. This sampling rate in time allows to detect and reasonably resolve the peak at the pulse frequency as is seen on the left plot in Fig. 4.

The selected sampling rate in time and space does not resolve the peak in the wakefield E_x behind the pulse. This is clear from the plot of its PSD shown in Fig. 4. In this plot, we zoomed at the domain close to the origin. The peak in the PSD of E_x is at the plasma frequency and wavevector which are much smaller than the wavevector and the frequency of the laser pulse field. The peak of the wakefield PSD can be resolved if we change appropriately the sampling rate in space and time and use sufficient number of sample points.

Results for the calculated pump depletion, using the described approach, for several runs with a Z_R ramp are summarized in Table 1. The pump depletion was calculated after

TABLE 1. Estimation of pump depletion and transverse leakage for laser pulse guiding in preionized channels. The estimates are from the total power spectral density calculated for runs in vacuum and for guiding in channels with one Rayleigh length ramp, wide and narrow transverse channel walls. The left column indicates the propagation distance. The notation nw corresponds to the narrow wall channel simulations.

Case	Pump depletion [%]	Leakage [%]
top of ramp	-0.1	≈ 0
Z_R inside channel	-0.8	-0.2
top of ramp, nw	-0.1	-0.1
Z_R inside channel, nw	-0.8	-0.9

a propagation length of one Rayleigh length in the ramp and after a Z_R in channels with wide and narrow walls. For both kind of channels, the pump depletion was estimated at 0.1 % after the pulse goes through the ramp and 0.8 % after one more Z_R in the channels.

The use of narrow wall channels is more efficient in the simulations since a much smaller number of plasma electrons have to be pushed. More importantly, transverse profiles of experimentally generated plasma channels for guiding show that the channel walls are not extended. Depending on the degree of preionization, the transverse plasma profile can be extended, if necessary. In narrow channels, there could be a neutral gas density in the wings of the channels that was not ionized during the channel creation. This gas could be field ionized by the wings of the pulse leading to additional pump depletion and leakage out of the channel. VORPAL simulations of this effect are underway and will be presented elsewhere.

The pump depletion results we obtained are of the same order of magnitude as from a simple theoretical calculation. Using Eq. (42) in Ref. [2] to calculate the pump depletion length for our pulse and plasma density wave parameters and assuming that the depletion varies linearly with the propagation length, we calculated the depletion through a Z_R propagation in plasma density of n_0 to be approximately 0.2 %.

The leakage out of the channel was calculated similarly to pump depletion except that the sum over lines with $y = const$ was limited to the region $-2W_0 \leq y \leq 2W_0$. This region contains the channel and extends over ± 2.8 standard deviations of the pulse transverse Gaussian profile (see Eq. (1)). The calculated total power spectrum is again compared to the total power spectrum for the same pulse in vacuum at its focus location and subtracted from the pump depletion calculated for the same propagation length. The data for leakage from the channel is also presented in Table 1. These results show that the leakage is higher for the narrow wall channel. The leakage from channels with too narrow walls could lead to a decrease in the efficiency of pulse guiding over many Rayleigh lengths compared to guiding in channels with wider walls.

While we have not completed the analysis of the large runs for channels with $3Z_R$ ramp lengths, the currently processed data shows that the leakage after Z_R and $2Z_R$ pulse propagation in the channel is several times larger than the leakage for the corresponding case with a Z_R ramp. The significantly increased leakage out of the channel for the longer length ramp show the importance of this parameter for efficient coupling of laser pulses

in preionized plasma channels and their subsequent guiding over many Rayleigh lengths. It is possible that adjusting the laser spot size at the top of the ramp could eliminate this enhanced leakage.

SUMMARY

We investigated the coupling of intense laser pulses to preionized plasma channels with 2D PIC simulations and a new FFT-based diagnostic that allows the detection of wavevector and frequency of propagating wave signals. This enables quantitative measurements of forward and backward propagating waves, including their energy and spectra.

We applied the FFT diagnostic to estimate pump depletion and transverse leakage from channels with different parameters. The results show that the length of the channel ramp and the width of its walls could significantly affect the coupling of a pulse to a channel. These results are of direct relevance to experimental design of plasma channels necessary to maximize the energy of electrons accelerated in a laser wakefield accelerator.

Future work will be directed toward VORPAL parameter studies designed to optimize the amount of laser energy that couples into a channel and on studying the effects of field ionization of neutral gas present in the region of the channel ramp and on the outside channel walls.

ACKNOWLEDGMENTS

The authors acknowledge helpful discussions with C. Nieter regarding the VORPAL code development. This work was supported by the US Department of Energy under contracts DE-FG03-02ER83557, DE-FC02-01ER41178, and use of NERSC supercomputer facilities.

REFERENCES

1. Nieter, C., and Cary, J. R., *J. Comput. Phys.*, **196**, 448–473 (2004).
2. Esarey, E., Sprangle, P., Krall, J., and Ting, A., *IEEE Trans. Plasma Sci.*, **PS-24**, 252 (1996).
3. Sprangle, P., Esarey, E., Krall, J., and Joyce, G., *Phys. Rev. Lett.*, **69**, 2200–2203 (1992).
4. Esarey, E., Sprangle, P., Krall, J., Ting, A., and Joyce, G., *Phys. Fluids B*, **5**, 2690 (1993).
5. Moloney, J., and Newell, A., *Nonlinear Optics*, Perseus Books, 2003, 3rd edn.
6. Bruhwiler, D. L., Giacone, R. E., Cary, J. R., Verboncoeur, J. P., Mardahl, P., Esarey, E., Leemans, W. P., and Shadwick, B. A., *Phys. Rev. ST Accel. Beams*, **4** (2001).